Boundary-Layer Meteorol (2012) 144:431–439
DOI 10.1007/s10546-012-9732-7

RESEARCH NOTE

First-Order Inconsistencies Caused by Rogue Trajectories

John V. Postma · Eugene Yee · John D. Wilson

Received: 24 January 2012 / Accepted: 24 April 2012 / Published online: 19 May 2012

Abstract A theoretical requirement of the Interaction by Exchange with the Conditional Mean (IECM) micromixing model is that the mean concentration field produced by it must be consistent with the mean concentration field produced by a traditional Lagrangian stochastic (LS) marked particle model. We examine the violation of this requirement that occurs in a coupled LS–IECM model when unrealistically high particle velocities occur. No successful strategy was found to mitigate the effects of these *rogue trajectories*. It is our hope that this work will provide renewed impetus for investigation into rogue trajectories and methods to eliminate them from LS models.

Keywords Lagrangian stochastic models · Micromixing models · Rogue trajectories

1 Introduction

Lagrangian stochastic (LS) trajectory models based on the "well-mixed condition" (WMC; Thomson 1987) have been used to simulate dispersion for a variety of source and flow configurations with good accuracy. Advantages of LS models over their Eulerian counterparts are: they are grid free and thus relatively simple mathematically and computationally; they can be run forward and backward in time; and (in contrast to eddy-diffusion closures) they correctly treat the near-field region of a source. Comprehensive reviews of LS trajectory models can be found in Rodean (1996) and Wilson and Sawford (1996).

J. V. Postma (✉) · J. D. Wilson
Department of Earth and Atmospheric Sciences, University of Alberta,
Edmonton, AB, T6G 2E3, Canada
e-mail: jpostma@ualberta.ca

E. Yee
Defence R&D Canada—Suffield, P.O. Box 4000,
Medicine Hat, AB, T1A 8K6, Canada

LS trajectory models are "driven" by a statistical description of the background velocity field. Improving the realism of the simulation by utilizing inhomogeneous (as opposed to simplified horizontally-homogeneous) driving velocity statistics is a promising approach to improve the predictions of LS trajectory models (e.g. Wilson et al. 2010). A complication arising from the use of more complex three-dimensional (3-D) flows is that the WMC no longer produces a unique LS model as it does in one dimension. Also, the larger gradients in the Reynolds stresses may promote the generation of unrealistically high velocities or *rogue trajectories* (e.g., Wilson and Yee 2000). However, rogue trajectories are also generated in one-dimensional LS models (e.g., Luhar and Britter 1989).

Yee and Wilson (2007) discussed in detail the cause of rogue trajectories and proposed a method for their prevention. In summary, rogue trajectories arise due to dynamical instabilities within the generalized Langevin equations whose expression depends on the fields of the mean velocities and Reynolds stresses. Furthermore, the simple forward Euler scheme commonly employed in LS models is unable to keep numerical round-off errors under control when integrating the stiff generalized Langevin equations. These two causes are related, with one exacerbating the other. They introduced a fractional-step semi-analytic integration scheme for the velocity fluctuation increment dU_i' that can, under certain conditions, prevent rogue trajectories from occurring but incurs the penalty that the LS model no longer satisfies the WMC. As this is undesirable, it is common to employ an ad hoc scheme to prevent or correct rogue trajectories: suppression of the velocity covariances, constraining the magnitude of the Eulerian velocity probability density function (PDF) or reinitializing the rogue trajectories based upon the local velocity statistics where they occur.

By coupling a LS trajectory model with the Interaction by Exchange with the Conditional Mean (IECM) micromixing model (Fox 1996; Pope 1998), predictions of the higher-order moments of the scalar concentration field can be made. A theoretical requirement of the IECM micromixing model is that the mean concentration field produced by it must be consistent with the mean concentration field produced by a LS trajectory model. Since the mean concentration is the first-order moment of the concentration field, this is referred to as the *first-order* consistency requirement. Recent applications of LS–IECM models to atmospheric flows include the simulation of dispersion in wall shear-layer flow (Cassiani et al. 2005a; Postma et al. 2011a), the convective boundary layer (Cassiani et al. 2005b; Luhar and Sawford 2005) and canopy flow (Cassiani et al. 2005c, 2007; Postma et al. 2011b). These studies all utilized simplified (e.g., horizontally-homogeneous) flow fields to drive the simulations that, for the studies by Postma et al, generated no rogue trajectories.

The simulations of dispersion into a canopy flow from line and localized sources (Cassiani et al. 2007; Postma et al. 2011b) generally underpredicted the mean concentration within the canopy, precisely where the assumption of horizontal homogeneity would be most tenuous. With an aim of improving the model predictions by increasing the realism of the driving flow field, a particular implementation of the LS–IECM modelling technique called Sequential Particle MicroMixing Model (SPMMM; Postma et al. 2011a) was driven by a more general inhomogeneous velocity field (i.e., the velocity statistics were allowed to vary in both the horizontal and vertical directions). The results (which are not reported in this study) broke the first-order consistency requirement of the IECM model. Closer examination showed that the locations of the first-order inconsistencies were coincident with locations that had a relatively large number of rogue trajectories. The process by which the first-order consistency requirement is broken is investigated in this study by using a greatly simplified flow field.

2 Model Formulation and Numerical Implementation

Full details of the governing equations and their numerical implementation in SPMMM can be found in Postma et al. (2011a). SPMMM couples a LS trajectory model,

$$\mathrm{d}U_i' = a_i(\boldsymbol{X}, \boldsymbol{U}', t)\mathrm{d}t + b_{ij}(\boldsymbol{X}, \boldsymbol{U}', t)\mathrm{d}\xi_j(t), \tag{1}$$

$$\mathrm{d}X_i = \left(\langle u_i \rangle + U_i'\right)\mathrm{d}t, \tag{2}$$

which governs the evolution of the Lagrangian velocity fluctuation relative to the Eulerian mean, $U_i' = U_i - \langle u_i \rangle$, and Lagrangian position X_i of a marked fluid parcel with the IECM micromixing model,

$$\mathrm{d}\phi = -\frac{1}{t_\mathrm{m}}(\phi - \langle \phi | \boldsymbol{u} \rangle)\mathrm{d}t, \tag{3}$$

which governs the evolution of the concentration ϕ of the marked fluid parcel. In the above equations dt is a small timestep calculated as $\mathrm{d}t = \mu_t \min[T_{L_u}, T_{L_v}, T_{L_w}]$, where $\mu_t \ll 1$ is the timestep constant and T_{L_u}, T_{L_v} and T_{L_w} are respectively the Lagrangian integral time scales associated with the streamwise, spanwise and vertical velocities. There are two terms on the right-hand side of Eq. 1: the deterministic drift term $a_i\mathrm{d}t$, and the stochastic diffusion term $b_{ij}\mathrm{d}\xi_j$. The deterministic drift coefficients a_i are modelled in accordance with Thomson's (1987) "simplest" (but not unique) solution for 3-D Gaussian turbulence (hereafter referred to as "Thomson-3D-G"). In the stochastic diffusion term, $\mathrm{d}\xi_j(t)$ represents an incremental Wiener process with zero mean and variance dt. Equation 3 has as a free parameter the scalar micromixing time scale t_m, and is modelled using inertial-subrange theory as originally proposed by Cassiani et al. (2005a). The mean scalar concentration conditioned on the local velocity (i.e., the conditional mean concentration) is denoted by $\langle \phi | \boldsymbol{u} \rangle$. If the gradients of the background velocity statistics (mean velocities, Reynolds stresses) are too large, the Thomson-3D-G solution (and SPMMM) may produce a rogue trajectory. In this study, a trajectory is considered unrealistic whenever a velocity fluctuation (in any direction) is greater than six times the local standard deviation ($U_i' > 6\sigma_i$). When this condition is encountered, the three components of the velocity fluctuation are randomly re-initialized according to the local velocity statistics.

SPMMM uses a pre-calculated conditional mean concentration field determined by a program called MEANS, which is a 3-D LS trajectory model based on the Thomson-3D-G solution. A residence time technique was used to calculate the conditional mean concentrations. MEANS releases from the source region a constant number of particles (N_ϕ), one at a time (i.e. independently), and records the total amount of time that particles spend in each bin of the discretized position-velocity space. From these total accumulated residence times $t_\mathrm{r}^v = t_\mathrm{r}^v(x_I, y_J, z_K, u_L, v_M, w_N)$, the conditional mean concentration for bin $(x_I, y_J, z_K, u_L, v_M, w_N)$ is calculated as

$$\langle \phi | \boldsymbol{u} \rangle = \langle \phi | \boldsymbol{u} \rangle(x_I, y_J, z_K, u_L, v_M, w_N) = \frac{Q t_\mathrm{r}^v}{\mathscr{V} N_\phi^v}, \tag{4}$$

where

$$N_\phi^v = N_\phi^v(x_I, y_J, z_K, u_L, v_M, w_N) = N_\phi f_{\boldsymbol{u}} \Delta u \Delta v \Delta w, \tag{5}$$

is the number of particles during the simulation that visit bin $(x_I, y_J, z_K, u_L, v_M, w_N)$, Q is the source strength, $f_{\boldsymbol{u}}$ is the PDF of the driving velocity statistics, and $\mathscr{V} = \mathscr{V}(x_I, y_J, z_K)$

is the volume of a spatial bin. With these pre-calculated conditional mean concentrations, SPMMM can simulate micromixing.

In SPMMM, particles are released (one at a time) from the upstream face of the spatial domain and allowed to propagate downstream. The initial positions of the particles are drawn from a uniform distribution. If a particle is initialized within the source region, then it is assigned a non-zero initial concentration, otherwise the initial concentration is zero. At each timestep, the concentration of the particle is compared to the conditional mean concentration calculated by MEANS and mixing occurs according to Eq. 3. At user-specified extraction locations, the concentration of the particle is saved to file for post-processing. When the particle leaves the simulation domain, the next particle is initialized and released. Once all the particle trajectories have been computed, the saved concentrations from the individual particles are averaged to produce mean concentrations at the data extraction locations.

Two simulations were performed for this study. The first, labelled as WSL (for wall-shear layer), used driving velocity statistics from wind-tunnel experiments for dispersion into a neutral wall-shear layer flow (Fackrell and Robins 1982). These were identical to those used by Postma et al. (2011a). As provided, these velocity statistics did not result in the generation of many rogue trajectories. The driving velocity statistics for the second simulation, labelled as ROG (for rogue), were identical to those of the WSL simulation except for the inclusion of a *rogue cell* in the volume bounded by $2.38 \leq x/\delta < 2.50$, $0.25 \leq y/\delta < 0.31$, and $0.50 \leq z/\delta < 0.53$ ($\delta = 1.2\,\text{m}$ is the boundary-layer depth). Within this volume, the variance of vertical velocity was artificially boosted by a factor of ten while ensuring that σ_w^2 remained differentiable in the discretized simulation domain. This resulted in large (but finite) streamwise, spanwise, and vertical gradients of σ_w^2 at this location that successfully produced rogue trajectories and in turn broke the first-order consistency requirement. This location was selected as it is on the edge of the plume where the mean concentration is lower and therefore is an ideal location to view the first-order inconsistency.

The details and the free parameters of the simulations were essentially identical to those used in Postma et al. (2011a). Only the source height ($h_\text{s} = 0.6\,\text{m}$) differed. This was to ensure that the particle reflection algorithm was not employed before the particles encountered the rogue cell, thus eliminating the reflection algorithm as a cause of the first-order inconsistency. Note, however, that the results presented herein do *not* depend on the values of the free parameters.

3 Results

3.1 Location of Rogue Trajectories and a First-Order Inconsistency

The particle step count for both the SPMMM-WSL and SPMMM-ROG simulations was approximately 1.2×10^9. Of these, the SPMMM-WSL simulation produced 27 rogue trajectories whereas the SPMMM-ROG simulation produced 16,582. Of these, 16,550 occurred within the rogue cell and the remaining 32 were scattered throughout the simulation domain. The effects of the recurring rogue trajectories on the first-order consistency between MEANS and SPMMM are shown in Fig. 1, which shows the spanwise transects of the mean concentration centred on the rogue cell. First-order consistency between MEANS-WSL and SPMMM-WSL is demonstrated in Fig. 1a. The small discrepancies between the two models are due to statistical noise. Within the rogue cell in Fig. 1b (between the dotted lines), the inconsistency in predicted mean concentration between MEANS-ROG and SPMMM-ROG is apparent.

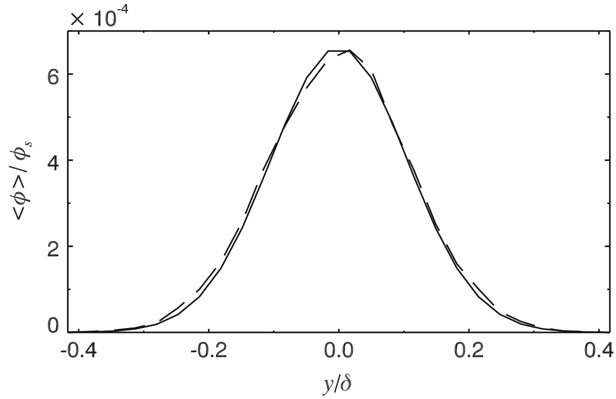

(a) WSL; simulation without the rogue cell

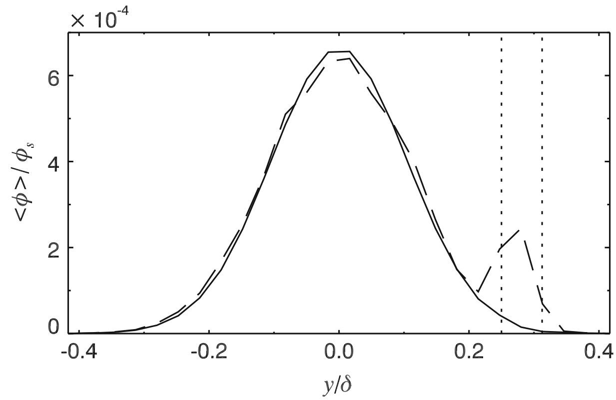

(b) ROG; simulation with the rogue cell

Fig. 1 Spanwise transects of the mean concentration centred on the location $(x/\delta, z/\delta) = (0.25, 0.50)$, corresponding to the upstream boundary of the rogue cell. The *top panel* displays the WSL simulation results and the *bottom panel* displays the ROG simulation results. The MEANS simulation results are represented by a *solid line*, while the SPMMM simulation results are represented by a *dashed line*. The *dotted lines* in the *bottom panel* demarcate the spanwise range of the rogue cell

Well outside this region, the discrepancies between MEANS-ROG and SPMMM-ROG are similar in magnitude to the discrepancies seen in the WSL simulation results. The strong correlation of the first-order inconsistency with a region of recurring rogue trajectories suggests that there is a causal relationship between the two.

3.2 Cause of the First-Order Inconsistency

The first-order inconsistency is a result of an incorrect accumulation of the conditional residence times by MEANS due to rogue trajectories. The end result was abnormally large conditional mean concentrations in areas with recurring rogue particles (i.e., near the rogue cell). The maximum conditional mean concentration experienced by particles in the SPMMM-ROG simulation was $\langle \phi | u, v, w \rangle / \phi_s \approx 0.61$, which was found within the rogue cell ($\phi_s \approx$

$4{,}900\,\mathrm{kg\,m^{-3}}$ is the source concentration). For comparison, regions outside the rogue cell in the SPMMM-ROG simulation had $\langle\phi|u, v, w\rangle/\phi_\mathrm{s} \lesssim 6.1\times10^{-4}$ which is 1,000 times smaller than the concentration within the rogue cell. Excluding the conditional mean concentrations found in the rogue cell, particles in the SPMMM-WSL and SPMMM-ROG simulations interacted with very similar fields of conditional mean concentration. When a particle from the SPMMM-ROG simulation mixes with the abnormally large $\langle\phi|u, v, w\rangle$ according to Eq. 3, its concentration increases dramatically. For example, a particle from the SPMMM-ROG simulation had its concentration increase from $\phi/\phi_\mathrm{s} \approx 6.1 \times 10^{-5}$ to $\phi/\phi_\mathrm{s} \approx 9.7 \times 10^{-3}$ in one timestep upon entering the rogue cell. For comparison, the maximum one-timestep concentration increase in the SPMMM-WSL simulation was $\Delta\phi/\phi_\mathrm{s} \approx 4.1 \times 10^{-5}$. Abnormally large particle concentrations are why the first-order inconsistency extends outside of the rogue cell in Fig. 1b; it takes time for the particle concentration to mix towards normal (i.e., those not affected by rogue trajectories) conditional mean concentrations.

The SPMMM-ROG simulation had 16,550 rogue trajectories occur within the rogue cell. The location in position-velocity space with maximum $\langle\phi|u, v, w\rangle/\phi_\mathrm{s} \approx 6.1 \times 10^{-1}$ corresponds to the single location that produced the most rogue trajectories (and, in particular, this single location generated 310 rogue trajectories). For convenience, this will be called the *maximal generating location*. Equation 5 predicts that, on average, two particles should have visited the maximal generating location for both simulations. In the SPMMM-WSL simulation, no particle visited this location, so the conditional residence time was $t_\mathrm{r}^v = 0$ and the conditional mean concentration was zero as a consequence. In contrast, in the SPMMM-ROG simulation, 310 particles (all of them rogue) visited the maximal generating location, the conditional residence time was $t_\mathrm{r}^v \approx 0.96\,\mathrm{s}$ and the conditional mean concentration was $\langle\phi|u, v, w\rangle/\phi_\mathrm{s} \approx 6.1 \times 10^{-1}$. This large conditional mean concentration is a result of a discrepancy between the normalization constant (which should be 2 as predicted by Eq. 5) and the number of particles accumulating conditional residence time (which in this case is 310, each of which corresponded to a rogue trajectory). Since the normalization constant is calculated using the PDF of the driving velocity statistics, and because this PDF cannot predict occurrences of rogue trajectories, there is a great mismatch between the accumulated residence time and the normalization constant. This results in Eq. 4 producing an abnormally large conditional mean concentration and ultimately resulting in the first-order inconsistency.

4 Discussion

The results shown in this work demonstrate that for flows with strong inhomogeneities, there are problems with rogue trajectories in the Thomson-3D-G solution, which forms the background in which the micromixing model operates. Reinitialization of the rogue trajectories did not significantly affect the predicted mean concentration of the LS model (MEANS results in Fig. 1b) but did significantly affect them for the LS–IECM model (SPMMM results in Fig. 1b). The cause of the first-order inconsistency discussed herein is specific to the SPMMM implementation that pre-calculates the conditional mean concentration field. However, it is conceivable that rogue trajectories could also affect other LS–IECM implementations. As atmospheric numerical models begin to make predictions of the higher-order concentration fluctuations, more attention will have to be paid to the effects of rogue trajectories. As was shown for SPMMM, re-initializing of rogue trajectories is not an acceptable solution.

4.1 Mitigation of Rogue Trajectories

An attempt to mitigate the effects of the rogue trajectories by an accurate accounting of the location of rogue trajectories in position-velocity space reduced the first-order inconsistency, but did not eliminate it. Since the rogue trajectories affect the accumulation of the conditional residence time and thus result in abnormally large conditional mean concentrations, the mitigation scheme is applied in MEANS by adding to Eq. 5 the total number of rogue trajectory occurrences for each bin in position-velocity space. Considering the results given above for the maximal generating location, the conditional residence time of $t_{\mathrm{r}}^{v} \approx 0.96\,\mathrm{s}$ would be normalized by 312 (=2 predicted by Eq. 5 + 310 rogue) particles as opposed to two particles under this mitigation scheme. The "corrected" conditional mean concentration was $\langle \phi | u, v, w \rangle \approx 4.3 \times 10^{-3}$ which, given that a first-order inconsistency still occurred within the rogue cell, was still too large. This mitigation scheme suffered from the finding that particles may not attain a rogue trajectory in one timestep, and may take two or three steps for a particle to become rogue (as defined by SPMMM). During these steps, which are not consistent with the velocity PDF and thus contaminate the predictions of Eq. 5, the velocity of the particle satisfied $U_i < 6\sigma_i$. Therefore the velocity of the particle is not re-initialized and no accounting of the location of these steps for use in the mitigation scheme is performed. Thus the first-order inconsistency persists. From a practical point of view, recording the location of rogue trajectories increased the computational requirements of SPMMM.

The first-order inconsistency is a result of rogue trajectories. Eliminate the rogue trajectories and the first-order inconsistency will be eliminated too. Additional SPMMM simulations performed with varying timesteps showed that the number of rogue trajectories decreased with decreasing timestep until $\mu_t = 0.02$, after which, further reductions in dt resulted in a slight increase in the number of rogue trajectories. For example, there were 70,913 rogue trajectories in the $\mu_t = 0.2$ simulation, 16,582 in the $\mu_t = 0.02$ simulation and 27,023 in the $\mu_t = 0.002$ simulation. Decreasing the timestep constant from $\mu_t = 0.2$ to 0.02 allows for a more accurate integration of the Langevin equations and therefore fewer rogue trajectories. However, simulations with smaller timesteps are more affected by round-off errors since dt itself is smaller (affecting all calculations involving it) and the increased number of particle steps that may result in the increased accumulation of round-off errors. These are believed to be the reasons that the $\mu_t = 0.002$ simulation produced more rogue trajectories than the $\mu_t = 0.02$ simulation.

Are rogue trajectories the result of intrinsic dynamical instabilities in the model, or, perhaps, the model dynamics are stable and the rogue trajectories are the result of using a poor integration routine to "follow" the model dynamics? If the former, then all implementations of LS–IECM models will be affected to some degree by rogue trajectories. If the latter, then perhaps improved integration procedures will give first-order consistency. The fractional-step semi-analytic integration scheme for the velocity fluctuation increment $\mathrm{d}U_i'$ introduced by Yee and Wilson (2007) splits the timestep into three steps. The first step integrates the constant, linear and stochastic contributions to $\mathrm{d}U_i'$; the second step integrates the diagonal terms of the non-linear contributions to $\mathrm{d}U_i'$; and the third step integrates the off-diagonal terms of the non-linear contributions to $\mathrm{d}U_i'$. If the third step of this integration scheme is omitted, then no rogue trajectories result through the integration of the generalized Langevin equations but at the cost that the model no longer (formally) satisfies the WMC. Given this, would it be useful to apply this integration scheme (omitting Step 3) in conjunction with MEANS and SPMMM, which guarantees the removal of rogue trajectories but at the cost that the model no longer (formally) satisfies the WMC?

Alternatively, Thomson-3D-G is not a unique solution. The WMC does not provide sufficient constraints on the model structure to produce a unique solution in three dimensions. Therefore, for a given velocity PDF, there are many different model structures that satisfy the WMC. Some of these model structures may exhibit dynamical instabilities and others may be dynamically stable. The former will probably give rise to rogue trajectories, as they are physically unreasonable. Given this, it should be possible to design a dynamically stable model that also verifies the WMC.

5 Summary

The generation of rogue trajectories by a discrete implementation of the Thomson-3D-G solution and their subsequent re-initialization breaks the theoretically required first-order consistency of the LS–IECM micromixing model SPMMM. This failure is specific to the pre-calculation algorithm employed by SPMMM, but it is conceivable that other numerical implementations of LS–IECM models, and perhaps other micromixing models that utilize LS models as the underlying basis for simulating the position and velocity of a marked fluid element may be affected by rogue trajectories. Of course, only further investigations with other models can address these questions.

The first-order inconsistency is a symptom of an underlying problem—the generation of rogue trajectories by the Thomson-3D-G solution. More research into the exact cause and prevention of rogue trajectories is needed. It is our hope that the results presented herein will provide renewed impetus for investigation into rogue trajectories and methods to eliminate them either through numerical means or alternative solutions that satisfy the WMC.

Acknowledgments This work was supported in part by grants from the Natural Sciences and Engineering Research Council of Canada (NSERC). We wish to thank the anonymous reviewers for their useful and constructive comments.

References

Cassiani M, Franzese P, Giostra U (2005a) A PDF micromixing model of dispersion for atmospheric flow. Part I: development of model, application to homogeneous turbulence and to a neutral boundary layer. Atmos Environ 39:1457–1469

Cassiani M, Franzese P, Giostra U (2005b) A PDF micromixing model of dispersion for atmospheric flow. Part II: application to convective boundary layer. Atmos Environ 39:1471–1479

Cassiani M, Radicchi A, Giostra U (2005c) Probability density function modelling of concentration in and above a canopy layer. Agric Forest Meteorol 133:153–165

Cassiani M, Radicchi A, Albertson JD (2007) Modelling of concentration fluctuations in canopy turbulence. Boundary-Layer Meteorol 122:655–681

Fackrell JE, Robins AG (1982) Concentration fluctuations and fluxes in plumes from point sources in a turbulent boundary layer. J Fluid Mech 117:1–26

Fox RO (1996) On velocity-conditioned scalar mixing in homogeneous turbulence. Phys Fluids 8:2678–2691

Luhar AK, Britter RE (1989) A random walk model for dispersion in inhomogeneous turbulence in a convective boundary layer. Atmos Environ 23:1911–1924

Luhar AK, Sawford BL (2005) Micromixing modelling of concentration fluctuations in inhomogeneous turbulence in the convective boundary layer. Boundary-Layer Meteorol 114:1–30

Pope SB (1998) The vanishing effect of molecular diffusivity on turbulent dispersion: implications for turbulent mixing and the scalar flux. J Fluid Mech 359:299–312

Postma JV, Wilson JD, Yee E (2011a) Comparing two implementations of a micromixing model. Part I: wall shear-layer flow. Boundary-Layer Meteorol 140:207–224

Postma JV, Wilson JD, Yee E (2011b) Comparing two implementations of a micromixing model. Part II: canopy flow. Boundary-Layer Meteorol 140:225–241

Rodean HC (1996) Stochastic Lagrangian models of turbulent diffusion. American Meteorological Society, Boston, 84 pp
Thomson DJ (1987) Criteria for the selection of stochastic models of particle trajectories in turbulent flows. J Fluid Mech 180:529–556
Wilson JD, Sawford BL (1996) Review of Lagrangian stochastic models for trajectories in the turbulent atmosphere. Boundary-Layer Meteorol 78:191–210
Wilson JD, Yee E (2000) Wind transport in an idealised urban canopy. In: Preprints, 3rd symposium on the urban environment. American Meteorological Society, pp 40–41
Wilson JD, Flesch TK, Bourdin P (2010) Ground-to-air gas emission rate inferred from measured concentration rise within a disturbed atmospheric surface layer. J Appl Meteorol Climatol 49(9):1818–1830
Yee E, Wilson JD (2007) Instability in Lagrangian stochastic trajectory models, and a method for its cure. Boundary-Layer Meteorol 122:243–261